Cell Host & Microbe
Resource

Cofactors Required for TLR7- and TLR9-Dependent Innate Immune Responses

Chih-yuan Chiang,[1,8] Alex Engel,[2,8] Amanda M. Opaluch,[1,8] Irene Ramos,[3] Ana M. Maestre,[3] Ismael Secundino,[4] Paul D. De Jesus,[1] Quy T. Nguyen,[1] Genevieve Welch,[6] Ghislain M.C. Bonamy,[6,7] Loren J. Miraglia,[6] Anthony P. Orth,[6] Victor Nizet,[4,5] Ana Fernandez-Sesma,[3] Yingyao Zhou,[6] Gregory M. Barton,[2] and Sumit K. Chanda[1,*]
[1]Infectious and Inflammatory Disease Center, Sanford-Burnham Medical Research Institute, La Jolla, CA 92037, USA
[2]Division of Immunology and Pathogenesis, Department of Molecular and Cell Biology, University of California, Berkeley, Berkeley, CA 94720-3200, USA
[3]Department of Microbiology and The Global Health and Emerging Pathogens Institute, Mount Sinai School of Medicine, New York, NY 10029, USA
[4]Department of Pediatrics
[5]Skaggs School of Pharmacy and Pharmaceutical Sciences
University of California, San Diego, La Jolla, CA 92093, USA
[6]The Genomics Institute of the Novartis Research Foundation, San Diego, CA 92121, USA
[7]Hudson-Alpha Institute for Biotechnology, Huntsville, AL 35801, USA
[8]These authors contributed equally to this work
*Correspondence: schanda@burnham.org
DOI 10.1016/j.chom.2012.02.002

SUMMARY

Pathogens commonly utilize endocytic pathways to gain cellular access. The endosomal pattern recognition receptors TLR7 and TLR9 detect pathogen-encoded nucleic acids to initiate MyD88-dependent proinflammatory responses to microbial infection. Using genome-wide RNAi screening and integrative systems-based analysis, we identify 190 cofactors required for TLR7- and TLR9-directed signaling responses. A set of cofactors were cross-profiled for their activities downstream of several immunoreceptors and then functionally mapped based on the known architecture of NF-κB signaling pathways. Protein complexes and pathways involved in ubiquitin-protein ligase activities, sphingolipid metabolism, chromatin modifications, and ancient stress responses were found to modulate innate recognition of endosomal nucleic acids. Additionally, hepatocyte growth factor-regulated tyrosine kinase substrate (HRS) was characterized as necessary for ubiquitin-dependent TLR9 targeting to the endolysosome. Proteins and pathways identified here should prove useful in delineating strategies to manipulate innate responses for treatment of autoimmune disorders and microbial infection.

INTRODUCTION

Vertebrates use interconnected branches of the immune system to dictate responses to commensal and pathogenic microbes and to maintain host health. In one strategy of immune sensing, invariant receptors, such as toll-like receptors (TLRs), are employed to recognize conserved molecules associated with microorganisms. Activation of these receptors allows cells to integrate contextual cues and signal for tissue repair, inflammation, and protective immunity (Kumar et al., 2011). Nucleic acid species are one class of microbial ligand sensed by multiple families of innate immune receptors.

The recognition of nucleic acids within endosomes is mediated by TLR3, TLR7/8, and TLR9, which sense double-stranded RNA (dsRNA), single-stranded RNA (ssRNA), and DNA, respectively (Blasius and Beutler, 2010). Many ssRNA, dsRNA, and dsDNA viruses have been found to activate endosomal TLRs, including human immunodeficiency virus (HIV), influenza virus, Sendai virus (SeV), and Newcastle disease virus (NDV) (Kawai and Akira, 2006; Melchjorsen et al., 2005; Paun et al., 2008). Furthermore, both bacterial and parasitic genomes can activate TLR7 and TLR9 (Arpaia et al., 2011; Takeuchi and Akira, 2010; Zinkernagel et al., 2011).

To sense pathogen infection, TLR7/9 must traffic from their site of synthesis in the endoplasmic reticulum (ER) to the endolysosomal network. Determinants for intracellular localization reside in both the transmembrane and cytosolic domains of these TLRs (Barton et al., 2006; Mouchess et al., 2011). The multipass transmembrane protein UNC93B1 is specifically required for endosomal TLR trafficking (Kim et al., 2008). During trafficking, TLR9 traverses the Golgi en route to acidified endolysosomes where it is proteolytically processed by cathepsins and asparagine endopeptidase to yield a functional N-terminally truncated receptor (Ewald et al., 2008; Park et al., 2008; Sepulveda et al., 2009). However, it remains unclear how sorting from the Golgi to the endolysosomal compartment is achieved. Intriguingly, the AP-3 complex, as well as protein-sorting complexes required for the formation of lysosome-related organelles, has been implicated in a late TLR9-trafficking event (Blasius et al., 2010; Sasai et al., 2010).

Unlike TLR3, both TLR7 and TLR9 signal through the adaptor MyD88 to produce either inflammatory cytokines or type I interferons (IFNs), depending on the cell type (Blasius and Beutler, 2010). In the proinflammatory arm of the signaling pathway, the

kinases IRAK1, IRAK2, and IRAK4 activate the E3 ubiquitin ligase TRAF6. Together with Ubc13 and Uev1A, TRAF6 catalyzes the K63-linked ubiquitination of substrates, including TRAF6 itself, as well as NEMO and TAK1. Ubiquitination of NEMO induces the formation of the IKK signalosome, where activated TAK1 phosphorylates IKK-β, leading to IκBα phosphorylation and degradation (Akira et al., 2006). This allows NF-κB to translocate to the nucleus and, with the transcription factor AP-1, activate proinflammatory cytokine production.

Ligand availability, receptor expression and localization, and downstream signaling networks are tightly regulated to effectively enable host defense while simultaneously limiting autoimmunity. To more comprehensively understand the molecular components that govern this process, we conducted a genome-wide RNAi analysis of the cellular requirements for endosomally initiated MyD88-dependent innate immune signaling. Integration of these results with orthogonal systems-based data sets yielded functional insight toward the regulatory hierarchies that preserve the critical balance between productive innate immune responses to pathogen challenge and hyperresponsiveness to autoantigens.

RESULTS

Genome-wide RNAi Analysis of MyD88-Dependent Endocytic Signaling

To establish a systems-level understanding of the compendium of genes that regulate innate immune responses to endosomal nucleic acids, we performed genome-wide RNAi screens to identify cofactors required for TLR7/9 signaling. To elucidate regulators of these pathways in a cell type that is tractable for high-throughput genetics, we selected HEK293T cells. Although these are not hematopoietic cells, they are able to recapitulate transcriptional responses to TLR ligands after constitution with appropriate receptors (Chuang and Ulevitch, 2004). To monitor activities of these innate pathways, HEK293T cells stably expressing either TLR7 or TLR9 were engineered to harbor an NF-κB luciferase reporter element (HEK293T/TLR7/NF-κB luciferase or HEK293T/TLR9/NF-κB luciferase reporter cell lines). Reporter cell lines were transfected with an arrayed genome-wide siRNA library targeting ~20,000 human genes (Konig et al., 2009). Subsequently, cells were stimulated with a synthetic TLR7 ligand, R848, or a TLR9 ligand, the CpG-containing oligonucleotide ODN2006-G5, and NF-κB luciferase activity was monitored (Figure 1A). We observed significant separation between positive and negative control siRNAs ($p < 10^{-100}$), and a large fraction of canonical TLR signaling components, including MyD88, IRAK1, TAK1, and IKK-α, were identified from the primary screen (Figure S1A and Table S1 available online, and data not shown).

Integrative Evidence-Based Analysis of Genome-wide RNAi Data Sets

Next, we used an integrative approach for candidate cofactor selection that considered additional lines of functional, biochemical, or transcriptional data (collectively called evidence-based analysis; see Figure 1A, Figure S1B, and the Supplemental Experimental Procedures). This approach is based on the assumption that a factor is more likely to be a physiologically relevant regulator of TLR signaling if multiple orthogonal lines of evidence can support experimentally derived RNAi activities. Thus, in addition to weighing individual well and multiple well RNAi activities for a gene (siRNA activity and RSA activity, respectively), we also considered if a candidate factor has a high level of reported protein interactions with other canonical or candidate innate immune factors (protein network), is expressed in relevant cell types, or is induced by TLR stimulation (gene expression) (Figure S1C) (Konig et al., 2007; Zhou et al., 2005). We combined these multiple lines of evidence into a weighted decision matrix and utilized a genetic algorithm to prioritize those factors that were the most likely to function as bona fide regulators of TLR signaling (Figures S1B and S1C, Table S2, and Supplemental Experimental Procedures).

This integrative evidence-based approach identified 546 genes as strongly supported candidate TLR7/9 cofactors. The activities of 190 cofactors were reconfirmed, employing criteria wherein each gene must be targeted by at least two sequence-independent siRNAs which attenuate R848- or CpG-mediated TLR signaling activation, while not significantly affecting cellular viability. These criteria significantly reduce, but do not eliminate, the possibility of RNAi-mediated off-target effects. Importantly, 80% of the known components of the TLR7/9 signaling pathways were identified in the primary screen and reconfirmed using these approaches (Table S1 and Table S2).

Gene ontology analyses of the 190 reconfirmed innate signaling cofactors revealed, as expected, enrichment of pathways and functions associated with innate immunity, including TLR and IL-1R signaling, innate responses to RNA viruses, NF-κB activation, and inflammation (Table S3). Furthermore, a collection of cofactors that are involved in chromatin modification, the sphingomyelin and ceramide synthesis pathways, and the unfolded protein response (UPR) were also enriched in this analysis (Figure S1D and Table S3). Significantly, 42 candidate cofactors could be genetically linked to multiple immune-related diseases through genome-wide association studies (GWAS) and expression analyses (Table 1 and Table S4).

To determine if the factors confirmed in the screen were expressed in cell types relevant to TLR7 and TLR9 surveillance activities, we extracted mRNA expression profiles from the GNF Tissue Atlas (Su et al., 2002). The expression of 67% of the confirmed cofactors could be detected in cells and tissues of myeloid and lymphoid origin, and more than 50% were predominantly expressed in hematopoietic cell types ($p < 3 \times 10^{-6}$), including plasmacytoid dendritic cells (pDCs) (Figure S1E). Furthermore, 30 of these genes were found to have highly significant expression correlation coefficients ($r^2 = 0.69$) with TLR7 and MyD88 (Figure 1B). Taken together, gene expression profiles of these identified molecules are largely consistent with their potential roles as TLR7/9 innate signaling cofactors.

We also evaluated the density of protein interactions between the 190 confirmed factors and known TLR signaling pathway members (see the Supplemental Experimental Procedures). This analysis identified a highly significant protein interaction network ($p < 0.001$) containing 105 total proteins and 85 confirmed gene products (Figure S1F). By expanding this network to include 546 primary screen hits, we generated an additional protein interaction network including 191 proteins and 109 confirmed factors (Figure 1C and Figure S1G). This interaction map reflects the probable biochemical hierarchies of innate

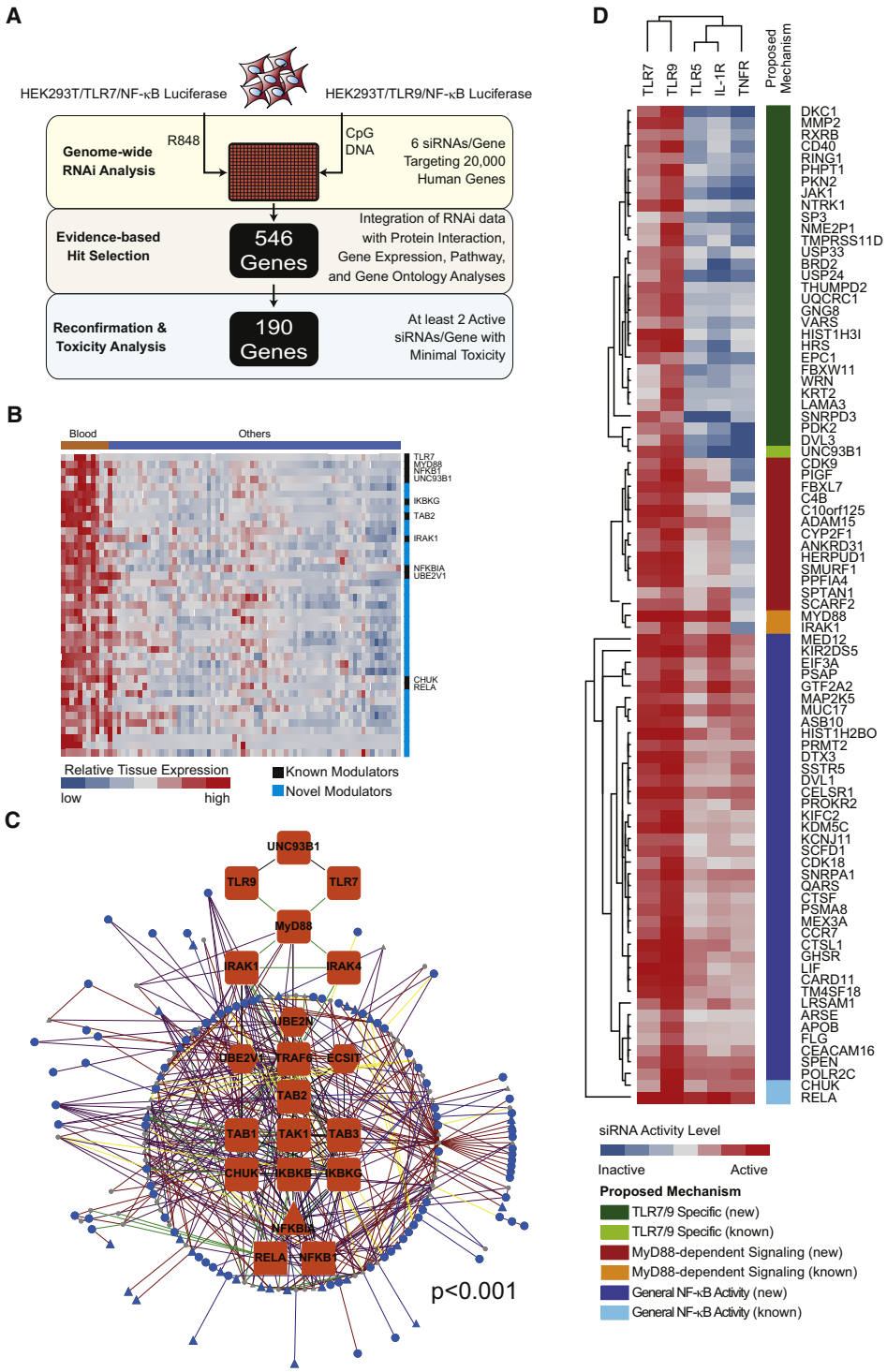

Figure 1. Genome-wide Integrative RNAi Analysis of TLR7- and TLR9-Mediated Innate Immune Responses

(A) HEK293T/TLR7/NF-κB or HEK293T/TLR9/NF-κB reporter cell lines were reverse transfected with an arrayed genome-wide siRNA library and stimulated with cognate ligands, and activation of the NF-κB pathway was monitored (yellow shaded area). Integration of these data with orthogonal systems-level data sets drove the selection of 546 genes (tan shaded area). One hundred ninety genes were subsequently confirmed to be required components of the TLR7 and/or TLR9 signaling response (blue shaded area).

(B) Tissue expression of 30 confirmed factors that have the strongest correlations with expression profiles of both TLR7 and MyD88. Tissues and cell types are depicted on the x axis (Blood, hematopoietic origin; Others, nonhematopoietic origin). Genes identified through the RNAi analyses are reflected on the y axis. Previously known or unknown pathway members are indicated by black or blue bars, respectively. A continuum of blue (low expression) to red (high expression) depicts relative expression levels.

Table 1. Confirmed Factors Involved in Autoimmune Diseases, Inflammatory Diseases, and Viral Infection

Disease	Analysis	TLR7/9 Signaling Cofactors	P Value
Systemic sclerosis	GWAS	RXRB, BRD2, RING1	0.000084
Systemic lupus erythematosus	GWAS	PHRF1	3.00E-10
	Expression profiling	EIF2AK2, PSMA6, UNC93B1, CTSL1, CASP3, TMUB2, MYD88, USP33, C6orf125, TLR7, PKN2	0.0333
Crohn's disease	GWAS	FUT2, LOC400456, CAPN10, CELSR1, GNAS, KRT2, LDLRAD1, LINGO2MAP2K5, MAST2, MKL2, MUC17, SMURF1, SP3, TRPC4AP, USP33, WRN	<9.7E-4
Multiple sclerosis	GWAS	CD40, BRD2	<9.712E-5
	Expression profiling	BCKDK, TBL3, POLR2I, PFKL, UNC93B1, ECSIT, RING1, MTMR14, COMT, KDM5C, HRS, RELA, MAP3K14, IKBKG, STK11, DVL1, POLR2C	0.0131
Inflammatory bowel disease	Expression profiling	ADAM15, KDM5C, MLL5, UNC13D, FBXW11, PIH1D1, BRD2, MMP2, WRN, PFKL, ACTN4, TEX264, MAP2K5, ANKRD31, CD40	0.000021
Rheumatoid arthritis	GWAS	CD40, ADRA1B, BRD2, APOB, C6orf125, CAPN10, GNAS, IL20RA, LAMA3, LINGO2, LRSAM1, MAST2, POLR2C, RING1	<9.7E-4
Systematic juvenile idiopathic arthritis	Expression profiling	NR4A2, ANPEP, UQCRC1, NFKBIA, KIFC2, BCKDK, COMT, PRDX5, VPS16, POLR2C, BRD2, FTL, PTPN6, MED30, GNAS	0.0232
Psoriasis	Expression profiling	KRT2, MYD88, CTSL1, TUBA3C, UBE2N, NFKB1, IRAK1, FLG, VCP, EIF3F, BRD2, GTF2A2, PSMA6, PSMA5, SPEN	0.0461
Staphylococcus aureus infection	Expression profiling	CCR7, NR4A2, LIF, EIF2AK2, CD40, NDP, RELA, NFKB1, CSF1, NFKBIA, UNC93B1, CTSL1, MYD88, PNRC1, DVL3	0.0067
Dengue virus infection	Expression profiling	C6orf125, VARS, CTSL1, HSP90B1, C1orf112, TBL3, RHBDD3, VCP, GHSR, MMP2, CAD, PHPT1, UQCRC1, POLR2I, SOX9	6.2E-10
Type I diabetes	GWAS	HIST1H3I, RXRB, VARS, BRD2, RING1, HIST1H2BO, C4B, MAP3K7, UBASH3A, C6orf125, LINGO2, VARS	<0.0125

References are contained in Table S4. Explanation of the column headings in table are as follows: Disease, name of the medical condition; Analysis, type of study conducted; TLR7/9 Signaling Cofactors, name of the cofactors that are associated with the disease; P Value, p value associated with that overlap.

immune regulatory proteins within the context of the canonical TLR7/9 signaling pathway. By identifying dense local interactions, our analysis also suggested that the identified regulatory proteins participate in higher-order biochemical interactions and protein complexes (Table S5 and Figures S1H–S1N).

Functional Classification of TLR7/9 Cofactors

To functionally characterize the regulatory role of 80 confirmed cofactors, we profiled their ability to modulate the NF-κB signaling pathway in response to ligand stimulation through TNF-α receptor (TNFR), IL-1β receptor (IL-1R), and TLR5. Based upon the known signaling architecture of these pathways, we were able to infer the likely impact upon individual steps of the TLR pathway for each gene (Figure 1D). RNAi against 29 genes, as well as *UNC93B1*, specifically impaired TLR7- and TLR9-mediated NF-κB activation, suggesting this category of genes may be involved in trafficking, processing, signaling, or transcriptional events associated specifically with TLR7/9 (Figure 1D; "TLR7/9 Specific"). RNAi against 13 genes, in addition to *MyD88* and *IRAK1*, impaired TLR5-, TLR7-, TLR9-, and IL-1R-mediated NF-κB activation, indicating that these genes are preferentially required for MyD88-dependent signaling responses (Figure 1D; "MyD88-dependent Signaling"). Finally, RNAi against 38 genes, as well as *IKK-α* and *p65*, impaired all interrogated receptor signaling pathways, implicating these genes in the global regulation of NF-κB-dependent responses (Figure 1D; "General NF-κB Activity").

Next, we manually curated the subcellular localizations and known functions of these 80 mediators of TLR7/9 signaling. This information was integrated with ligand profiling data

(C) The network relationship between identified innate regulators and the canonical TLR7/9 signaling components is depicted. (Interaction type, protein type, and expression patterns are distinguished by differential edge color, node color, and node shape, respectively, as indicated in Figure S1G.)
(D) Confirmed TLR7/9 signaling cofactors were crossprofiled for their activities upon TLR5-, TLR7-, TLR9-, TNFR-, and IL-1R-mediated induction of a NF-κB-dependent reporter. Data used to generate the heat map depicted in (D) are representative of duplicate assays, with three wells per gene tested in each assay. Also see Figure S1.

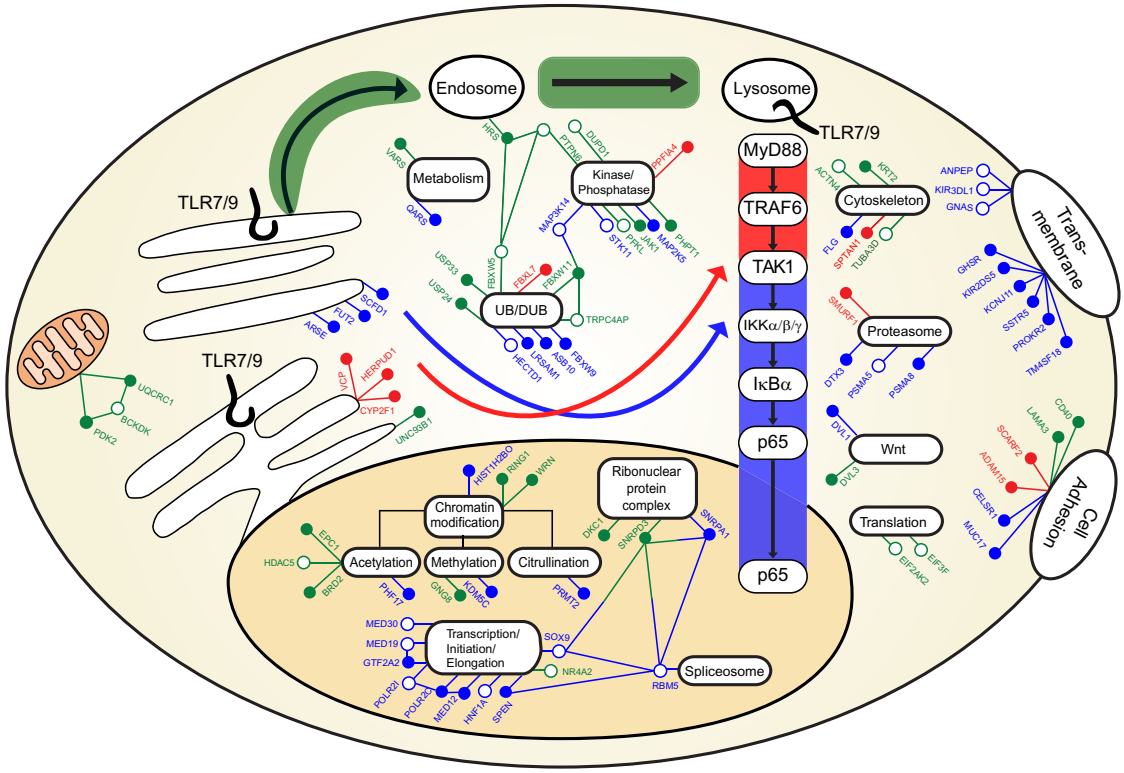

Figure 2. Comprehensive Model of Functional and Regulatory Roles of Confirmed TLR7/9 Cofactors

Subcellular localization and functional data for identified innate regulators were curated using multiple databases (Table S6). Innate cofactors were mapped to their likely regulatory roles in TLR7 and TLR9 signaling (solid circles). SVM-based gene regulatory activity predictions are also depicted (open circles) (see Table S6). TLR7/9-specific factors are represented by green nodes, MyD88-dependent factors are indicated by red nodes, and regulators of general NF-κB activation are shown as blue nodes. Lines between proteins predict biochemical interactions (see Figure 1D).

(Figure 1D) and protein interaction data (Figures S1F and S1G) to construct a comprehensive model that reflects the likely functional and regulatory intersections between the innate signaling molecules identified here and the canonical TLR7/9 pathway (Figure 2 and Table S6; also see the Supplemental Experimental Procedures).

Molecular and Biochemical Analyses of Confirmed Cofactors

Subsequently, to verify that depletion of the confirmed innate cofactors impacted the transcriptional response to TLR ligands, we profiled the role of these factors in the induction of NF-κB-dependent target genes. Silencing of >80% of confirmed factors in HEK293T cells reduced *IL-8* target gene induction (Figure S2A and Table S7). Furthermore, of the 91 genes found to most potently regulate TLR7/9 responses, inhibition of 78 genes (85.7%) decreased R848-induced *ICAM-1* mRNA expression in THP-1 monocytic cells (Figure 3A, Figures S2A and S2B, and Table S7). Importantly, these data demonstrate that the cofactors identified by our analysis impact innate immune signaling in a myeloid-lineage cell line.

Next, we measured the effects of siRNA-mediated depletion of confirmed factors upon R848-induced p65 nuclear translocation. An evaluation of both target gene data and p65 localization data allowed us to distinguish between innate cofactors with nuclear versus cytoplasmic activities (Figures S2A and S2C, and Table S7). For example, siRNAs targeting several mitochondrial-, ER-, or cytoplasmic-localized proteins impaired not only *IL-8* mRNA expression but also p65 nuclear translocation, suggesting these genes regulate upstream TLR signaling events. In contrast, siRNAs targeting a group of nuclear localized proteins inhibited *IL-8* mRNA expression while p65 nuclear translocation remained intact, providing evidence to support a role for these genes in transcriptional or epigenetic control of the inflammatory response (Figure 2).

Finally, we tested a subset of confirmed TLR7/9 cofactors for their ability to regulate the endosomal response to SeV infection. Since SeV robustly induces a RIG-I-mediated immune response (Melchjorsen et al., 2005), we evaluated the cofactors in a RIG-I-deficient background. Silencing of *TLR7*, *UNC93B1*, or *MyD88* significantly reduced induction of NF-κB by SeV, indicating a TLR7-dependent response to infection (Figure 3B). Notably, we observed that silencing of 7 out of 12 selected cofactors significantly attenuated immune responses to SeV infection (Figure 3B, data not shown).

In an effort to test predicted pathway activities and protein interactions for innate signaling cofactors (Figure 1C and Figures S1F and S1G), we selected a small subset of genes for coimmunoprecipitation analysis (Figure 3C). We found that ~50% of these selected cofactors physically associated with the canonical

TLR pathway member predicted by our protein-protein interaction analysis (Figure 3C and Figure 4A; data not shown). For example, protein network analyses suggested that pyruvate dehydrogenase kinase, isozyme 2 (PDK2) physically interacts with TRAF6, Uev1A, Ubc13, and TAK1 through an intermediate protein (Figure 1C and Figure S1G); coimmunoprecipitation confirmed that PDK2 does physically associate with both TRAF6 and TAK1, although we were unable to detect a physical interaction between PDK2 and Uev1A or Ubc13 (Figure 3C). In addition, PDK2 depletion inhibited ligand-induced expression of IL-8, p65 nuclear translocation, and altered IκBα degradation kinetics (Figures 3D–3F, Figure S2D); this suggests that PDK2 functions upstream of IKK activation, and is consistent with the predicted PDK2 activity derived from ligand profiling studies (Figure 1D). Additional coimmunoprecipitation experiments revealed biochemical interactions between the ubiquitin protein ligase, FBXL7 (F box and leucine-rich repeat protein 7), and TLR7/9 pathway members IRAK1, TRAF6, and TAK1, which are all known be modified by ubiquitin following receptor activation (Conze et al., 2008; Takeuchi and Akira, 2010) (Figure 3C). Interestingly, we observed that TLR pathway members interacted with expected (~54 kDa) and higher molecular weight forms of FBXL7, suggesting that this F box protein may be subject to posttranslational modification. Since depletion of FBXL7 also impaired IκBα degradation kinetics, p65 nuclear translocation, and IL-8 upregulation (Figures 3D–3F, and Figure S2E), our data suggest that FBXL7 may be a MyD88-dependent regulator of ubiquitination events that occur prior to the activation of the IKK signalosome complex.

Finally, coimmunoprecipitation experiments using ectopically expressed tagged TLR9 and HRS revealed that TLR9 interacted with HRS, and the affinity of HRS for TLR9 was stronger than its affinity for cell-surface-expressed TLR2 (Figure 4A). Taken together with data demonstrating that HRS was uniquely required for endosomal signaling (Figure 1D and Figure 2), this finding was of particular interest, since HRS has been shown to mediate plasma membrane-associated receptor trafficking toward the lysosome (Saksena et al., 2007; Wegner et al., 2011).

A Role for HRS in Endosomal TLR Trafficking

To pursue the hypothesis that HRS might play a role in targeting TLR7/9 to the endolysosomal compartment, we verified depletion of HRS protein and further assessed the impact of HRS on NF-κB signaling (Figure S3A). In HRS-depleted cells, NF-κB promoter activation was significantly reduced after stimulation with R848 or CpG, but remained intact after stimulation with TNF-α (Figure 4B). Furthermore, R848-induced secretion of IL-8 was abrogated with *HRS* knockdown in HEK293T cells (Figure 4C), and *HRS* silencing in THP-1 cells reduced target gene induction in response to TLR7 ligand, but not TNF-α, or the TLR2 agonist Pam3CSK4 (Figure S3B). *HRS* knockdown in HEK293T cells also resulted in the blockage of p65 nuclear translocation in response to R848, as well as the impairment of ligand-mediated IκBα degradation (Figures 4D and 4E). Importantly, silencing of *HRS* in primary macrophage-derived dendritic cells (MDDCs) reduced TLR-dependent induction of *TNF-α* and *IFN-α* following infection with NDV (Figure 4F), underscoring the critical role of HRS in the endosomal innate response to virus infection. Together, these results indicate that HRS specifically regulates TLR7/9-initiated signaling events that occur prior to TAK1 activation, and are consistent with a role for HRS in endosomal receptor trafficking.

When delivered to acidified endosomal compartments, TLR9 (150 kDa) is proteolytically processed, generating an ~80 kDa cleaved species that is a hallmark of proper TLR9 trafficking (Ewald et al., 2008; Park et al., 2008). Furthermore, in the absence of the trafficking chaperone UNC93B1, no cleaved TLR9 species is observed (Figure 5A). In order to evaluate if HRS was required for this endosomal trafficking event, we examined whether TLR9 was properly cleaved following HRS knockdown. Silencing of *HRS* in a RAW264.7 cell line resulted in a 70% reduction of HRS protein levels, which corresponded to an ~60% decrease in the abundance of cleaved TLR9 (Figure 5A). Thus, these data support an essential role for HRS in TLR9 receptor trafficking.

It has been previously shown that HRS recognizes ubiquitinated cargo (Saksena et al., 2007). Because HRS physically interacts with TLR9 and is required for endolysosomal localization of the receptor, we investigated the role of TLR9 ubiquitination in receptor trafficking. When TLR9 was immunoprecipitated from immortalized macrophages or RAW264.7 cells expressing wild-type (WT) TLR9-HA, a high molecular weight ubiquitinated species was detected (Figure 5B and data not shown). Mutation of the three lysine residues in the cytosolic linker and TIR (toll IL-1 receptor) domain of murine TLR9 (K878, K932, K963, called "TLR9 KallR mutant") resulted in a highly significant reduction in the amount of ubiquitin staining in the TLR9 immunoprecipitate, suggesting that TLR9 is directly ubiquitinated (Figure 5B). Since HRS binds ubiquitinated cargo at the surface of early endosomes, we evaluated whether TLR9 ubiquitination might occur at this location (Saksena et al., 2007). In MEF cell lines, ectopic expression of UNC93B1 is required for the exit of TLR9 from the ER (Ewald et al., 2008). Consistent with ubiquitination of TLR9 in a post-ER compartment, coexpression of UNC93B1 was required for ubiquitination of TLR9 (Figure 5C). This UNC93B1-dependent ubiquitination also required TLR9 cytoplasmic lysines. Importantly, we find that while WT TLR9 strongly interacted with HRS, the TLR9 KallR mutant exhibited a very low affinity for HRS, suggesting that HRS specifically binds the ubiquitinated receptor (Figure 5D).

To determine the functional relevance of TLR9 ubiquitination for signaling, we stimulated *TLR9*$^{-/-}$ immortalized macrophages expressing single, double, and triple lysine-substituted constructs and measured the production of TNF-α. Whereas WT TLR9 and TLR9-K878,963R were able to robustly produce TNF-α in response to CpG-B oligonucleotides, signaling by TLR9-K932R was strongly diminished, and the TLR9 KallR mutant was completely defective for signaling (Figure 5E). Though TLR9 K932 is strongly conserved across all TLR family members (Figure S4A), this lysine is not universally required for TLR signaling, as an analogous substitution in TLR2 (K698R) did not alter responsiveness to Pam3CSK4 (Figure S4B). However, substitution of two corresponding lysines in TLR7 (K952 and K953) reduced R848-mediated signaling, possibly reflecting an important and unique role for ubiquitination of these lysines in endosomal TLR function (Figure S4C).

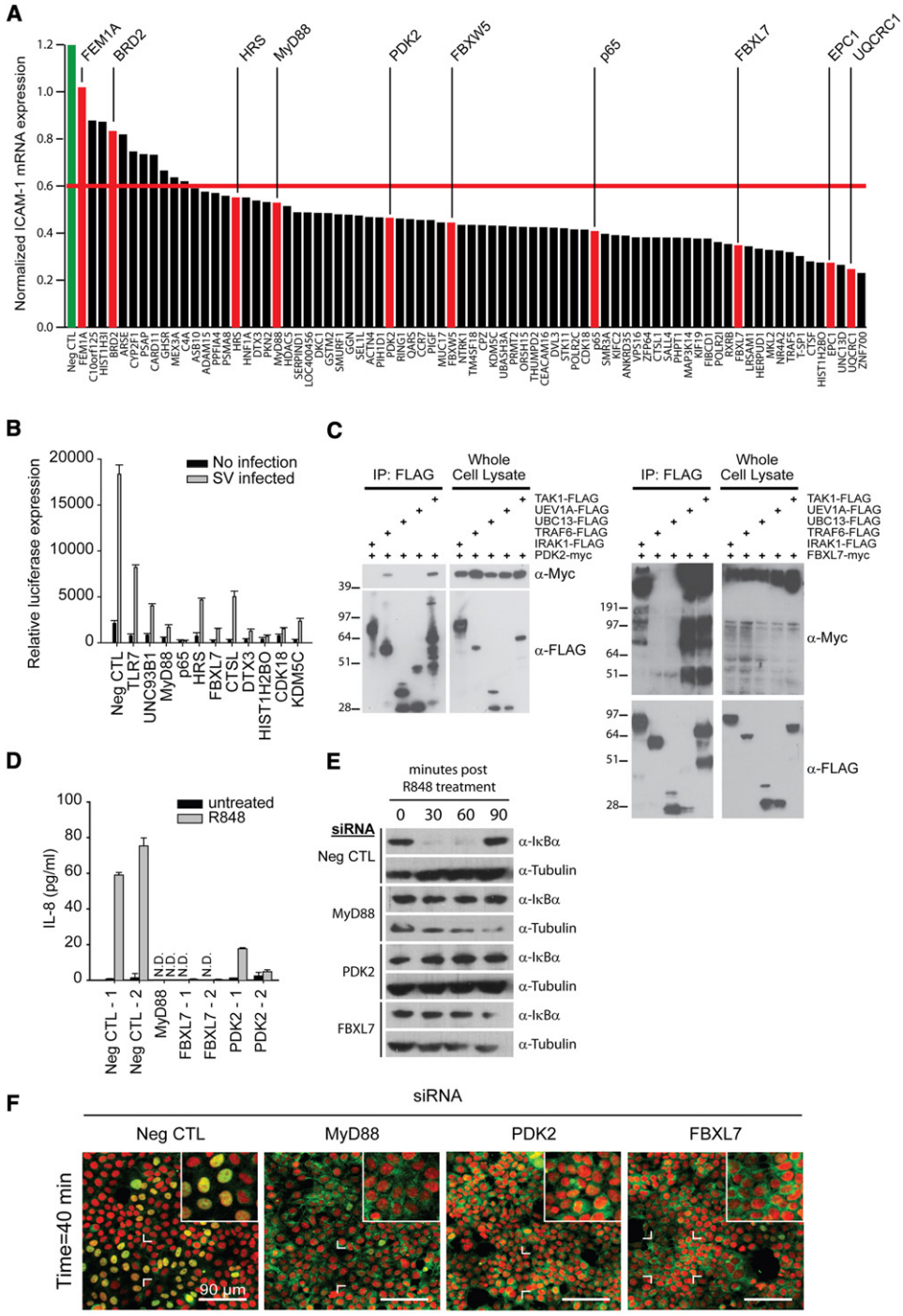

Figure 3. Characterization of Selected Confirmed Genes onto the TLR Signaling Pathway

(A) THP-1 cells were transfected with indicated siRNAs and stimulated with 5 μM of R848. Five hours poststimulation, mRNA levels of *ICAM-1* were quantified by RT-PCR. The red bar reflects a threshold at which 50% of the *ICAM-1* mRNA expression was inhibited compared to the negative control (Neg CTL) siRNA.

(B) HEK293T/TLR7/NF-κB reporter cells were transfected with the indicated siRNAs together with an siRNA targeting *RIG-I* and infected with Sendai virus, and luciferase reporter activity was quantified.

(C) HEK293T cells were cotransfected with indicated expression vectors. Whole-cell lysates (WCLs) were immunoprecipitated using FLAG antibody. Immunoprecipitatants were assayed by western blot analysis using FLAG or Myc antibodies.

(D) HEK293T/TLR7/NF-κB reporter cells were transfected with indicated siRNAs and stimulated with 3 μM R848 for 12 hr, and secreted IL-8 was quantified by ELISA.

(E) HEK293T/TLR7/NF-κB reporter cells were transfected with indicated siRNAs. Cells were stimulated with 10 μM of R848, and WCLs were immunoblotted with antibodies against IκBα and tubulin.

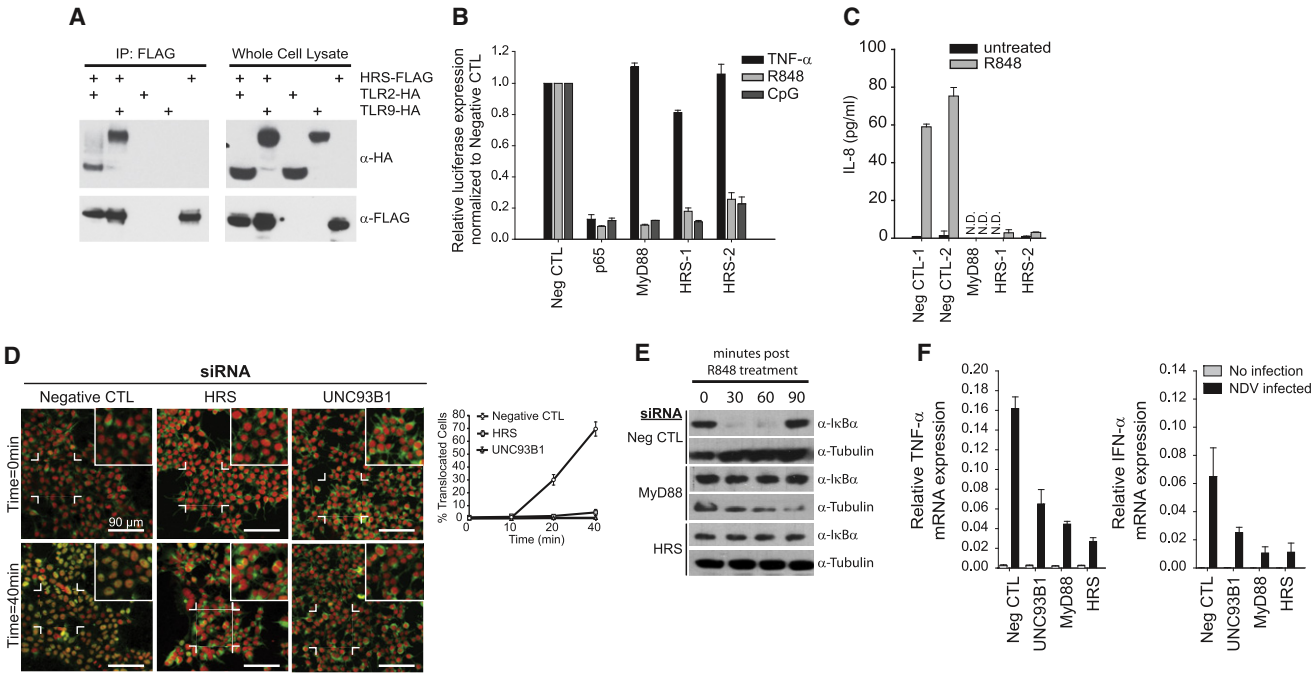

Figure 4. HRS Regulates TLR7 and TLR9 Signaling

(A) HEK293T cells were cotransfected with the indicated expression vectors. WCLs were immunoprecipitated using FLAG or IgG (data not shown) antibodies. Immunoprecipitatants were assayed for western blot analysis using FLAG or HA antibodies.

(B) HEK293T/TLR7/NF-κB or HEK293T/TLR9/NF-κB reporter cells were transfected with the indicated siRNAs. After stimulation with 0.5 μM of R848, 3 μM of CpG DNA, or 10 ng/ml of TNF-α, NF-κB luciferase reporter activity was quantified.

(C) HEK293T/TLR7/NF-κB reporter cells were transfected with indicated siRNAs, and secreted IL-8 was quantified by ELISA.

(D) Cells were transfected with siRNAs as in (C), and p65 localization was detected and quantified (green, p65; red, nucleus).

(E) HEK293T/TLR7/NF-κB reporter cells were transfected with siRNAs against *HRS*. WCLs were harvested and immunoblotted with antibodies against IκBα and tubulin.

(F) Human MDDCs were cotransfected with indicated siRNAs and an siRNA targeting *RIG-I* and were subsequently infected with NDV. *TNF-α* and *IFN-α* mRNA levels were quantified by RT-PCR. Silencing of *MyD88*, *UNC93B1*, and *HRS* was also verified by RT-PCR (silencing of >50% for each gene, data not shown). Data shown in (A)–(E) are representative of n = 3 experiments. Data shown in (F) are representative of two individual donors. Data in (B) are presented as percent relative to negative control siRNAs ± SD. Data in (C), (D), and (F) are presented as mean ± SD from a representative experiment. Also see Figure S3.

TLR9 has recently been shown to contribute to the macrophage innate immune response against Group A *Streptococcus* (GAS) (Zinkernagel et al., 2011). To evaluate the function of TLR9 ubiquitination in the innate response to pathogen challenge, WT TLR9-HA or TLR9 KallR-HA macrophages were infected with GAS (Simon and Ferretti, 1991), and intracellular bacterial killing was evaluated (Figure 5F). TLR9 KallR-HA macrophages showed reduced ability to control intracellular replication of GAS compared to WT TLR9-HA macrophages, suggesting that ubiquitination of TLR9 cytoplasmic lysines is critical for pathogen sensing.

Finally, we monitored processing of TLR9 mutants to evaluate whether proper trafficking of these nonubiquitinated receptors occurred. A high percentage of cleaved product was observed for both WT and TLR9-K878,963R constructs, while very little cleaved product was observed for the TLR9-K932R and TLR9-KallR mutants (Figures 5G and 5B), suggesting the signaling defect of these mutants could be attributed to failed sorting. Importantly, a fraction of full-length TLR9 KallR protein was insensitive to digestion with the glycosidase EndoH, indicating that this mutant does exit the ER and reach the Golgi compartment (Figure S4D). Additionally, we assessed trafficking of TLR9 by purifying phagosomes and immunoblotting for the presence of TLR9. The cleaved form of WT TLR9 was exclusively detected in the purified phagosome preparation, while neither full-length nor cleaved TLR9 KallR was detected (Figure 5H). In agreement with phagosomal localization, WT TLR9 strongly colocalized with the late endosomal marker LAMP-1 (70/70 cells), whereas only 20% of TLR9-KallR mutants displayed strong colocalization (n = 70) (Figures S4E and S4F). Taken together, these results suggest that HRS regulates the ubiquitin-dependent delivery of TLR9 to endolysosomes and phagosomes (Figure S4G).

(F) HEK293T/TLR7/NF-κB reporter cells were transfected with indicated siRNAs, and p65 localization was detected and quantified (green, p65; red, nucleus). The experiments for Figure 4E and (E) were performed concurrently, and the Neg CTL and MyD88 blots are shared between the two figures. The experiments for Figure 4C and (D) were performed concurrently, and the Neg CTL and MyD88 data are shared between the two figures. All data shown are representative of n = 3 experiments. Bar graphs in (B) and (D) are presented as mean ± SD from a representative experiment. Also see Figure S2.

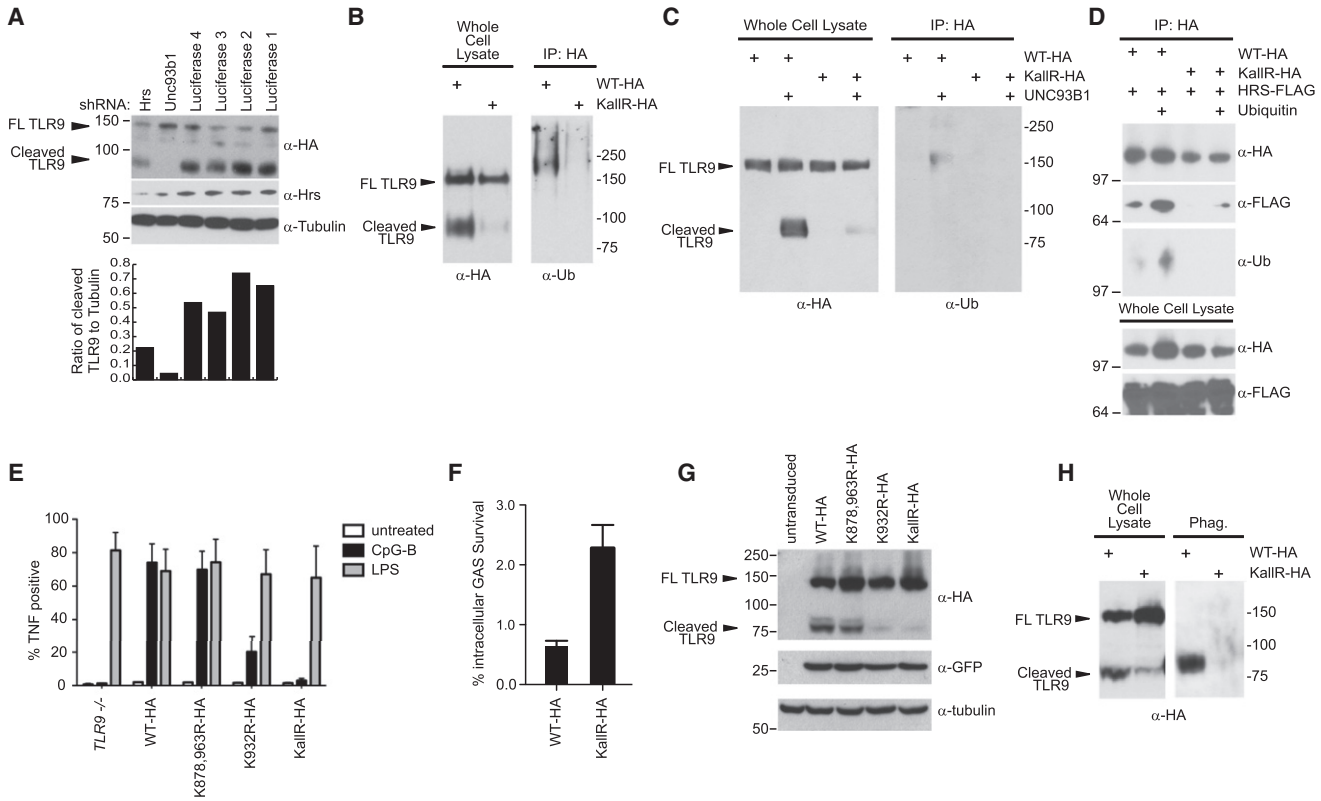

Figure 5. TLR9 Ubiquitination, Signaling, and Cleavage Are Dependent on TLR9 Cytoplasmic Lysines

(A) RAW264.7-TLR9-HA cells were transduced with the indicated shRNAs. WCLs were harvested and immunoblotted with antibodies against HA, HRS, or tubulin. The ratio between cleaved TLR9 and tubulin was quantified by densitometry.

(B) WCLs from *TLR9*$^{-/-}$ immortalized macrophages expressing either WT-TLR9-HA or KallR-TLR9-HA were subjected to immunoprecipitation using HA antibodies and assayed by western blot analysis with the indicated antibodies.

(C) UNC93B1 was coexpressed with WT-TLR9-HA and KallR-TLR9-HA in *TLR9*$^{-/-}$ MEF cell lines. WCLs were immunoprecipitated with HA antibodies and assayed by western blot analysis with the indicated antibodies.

(D) HEK293T cells were cotransfected with the indicated plasmids, and WCLs were subjected to immunoprecipitation using anti-HA beads or IgG antibodies (data not shown). Proteins were detected by western blot analysis using antibodies against HA, FLAG, or ubiquitin.

(E) Cell lines described in (B) were stimulated with the indicated TLR ligands, and intracellular TNF-α was quantified. Data shown are the percent of total live cells present in the TNF^{+} gate for a representative experiment.

(F) Cell lines described in (B) were infected with GAS, and intracellular bacteria content was quantified.

(G) Western blot analysis of WCLs from (E).

(H) Purified phagosomes/endolysosomes were assayed by western blotting with an anti-HA antibody. Data shown in (A)–(E) and (G) and (H) are representative of n = 3 experiments. Data shown in (F) are representative of n = 2 experiments, each done in triplicate. Bar graphs in (E) and (F) are presented as mean ± SD from a representative experiment. Also see Figure S4.

DISCUSSION

Here, we describe a genome-wide analysis of the cofactors that are required for MyD88-dependent endosomal innate signaling. By integrating orthogonal systems-level approaches, including RNAi data, cellular protein-protein interaction network analyses, and gene expression profiling data, we were able to identify and confirm 190 cofactors that mediate TLR7/9 signaling responses. Based on the activity of the confirmed factors in response to TLR5, TLR7, TLR9, TNFR, and IL-1R stimulation, we categorized a subset of genes as three different types of NF-κB regulators: TLR7/9 specific, MyD88-dependent signaling, and general NF-κB activity. Using these functional predictions, we were able to further classify an additional 38 candidate innate regulatory factors using a support vector machine (SVM) algorithm (Figure 2 and Table S6; also see the Supplemental Experimental Procedures). Finally, these data were consolidated to construct a comprehensive predictive model that defines the likely regulatory hierarchies of the identified innate regulatory genes during the innate response to pathogen challenge.

Transcriptional Control of the Inflammatory Response through Chromatin Remodeling

Histones are subject to posttranslational modifications that govern gene expression through the remodeling of global chromatin environments (Kouzarides, 2007). Interestingly, we found that several chromatin modifiers were involved in the regulation of general proinflammatory responses. For example, PRMT2, HDAC5, and PHF17 affected NF-κB activation in response to all ligands tested. This suggests that these proteins facilitate

the maintenance of chromatin conformations that enable rapid transcriptional responses to proinflammatory stimuli.

However, we also identified chromatin-modifying factors, such as BRD2, EPC1, GNG8, and WRN, that have activities specific for only TLR7- or TLR9-mediated NF-κB transcriptional activation. Consistent with a role in directing epigenetic modifications in response to endosomal TLR activation, we find that in cells depleted of the TLR7/9-specific chromatin-modifying factors identified here, ligand-induced upregulation of *IL-8* mRNA is impaired, while p65 nuclear translocation is unimpeded; this suggests that the chromosomal architecture of NF-κB target genes may be regulated in a ligand-dependent manner, and that upstream pathway regulators may be able to encode stimulus-specific information that is transmitted to the downstream transcription machinery. Importantly, such activities may enable overlapping, but unique, transcriptional responses driven by a variety of proinflammatory stimuli. Taken together, these results may provide insight into the mechanisms by which different pattern recognition receptors are able to utilize shared pathway architectures to mediate distinct innate immune transcriptional responses.

Sphingolipid Metabolism Contributes to TLR-Mediated Proinflammatory Signaling

Sphingolipid synthesis and metabolism are critical for the formation of cellular membranes, lipid rafts, and the generation of second lipid messenger ceramide; importantly, these pathways have previously been linked to induction of immune responses (Cinque et al., 2003). Here, we have found a significant enrichment of genes involved in both ceramide and sphingomyelin synthesis ($p < 2 \times 10^{-4}$) (Table S3; HNF1A, PROKR2, PSAP, CXCR1, FLG, and APOB) to be required for TLR-, IL-1R-, and TNFR-mediated NF-κB activation, further underscoring the connection between lipid metabolism and innate immune signaling. Ceramide and sphingomyelin have been shown to be agonists for MAPK, AP-1, or NF-κB activation in the absence of other environmental stimuli (Cinque et al., 2003), and our results indicate that the endogenous sphingolipid metabolism is an important component of TLR-mediated activation of innate target genes. Consistent with our observations, treatment with D609 (an inhibitor of PC-PLC, which regulates acid sphingomyelinase) has been shown to protect mice from septic shock, suggesting that lipid metabolism is intricately linked to the efficient production of proinflammatory cytokines by TLRs (Machleidt et al., 1996). Importantly, our results indicate that this metabolic pathway is an integral component of the general NF-κB signaling response to pathogen challenge, since all ceramide metabolism-associated genes identified by RNAi analysis affected NF-κB activation in response to all stimuli tested.

Involvement of Organelles and Ancient Stress Responses in TLR7/9 Signaling

Organelles support general cell homeostasis through specialized functions but can also serve as platforms for signal initiation or as points of integration. Indeed, organelle-bound proteins are associated with pathways governing ancient stress responses, including the glycolytic pathway, the UPR, and innate immunity. For example, innate responses mediated by the cytosolic PRR, RIG-I, are dependent on the mitochondrial membrane protein, MAVS (Seth et al., 2005; Yoneyama et al., 2004). The present study has identified genes that are associated with the mitochondria, suggesting the existence of a parallel innate signaling circuit that routes through this organelle. Additionally, we have also found a number of genes that participate in ER-associated UPR, as well as factors that localize to the Golgi (see Figure 2 and Table S3).

In times of cellular stress or danger, limited ambient oxygen results in a switch to mitochondrial energy production by anaerobic glycolysis, a process that is primarily governed by posttranslational regulation of hypoxia-inducible factor-1 alpha (HIF-1α) (Carmeliet et al., 1998; Maxwell et al., 1999). Importantly, several studies have provided compelling evidence to support an intricate relationship between this hypoxic response and innate immunity (Tannahill and O'Neill, 2011). Here, we find that the glycolytic enzyme PDK2 and a component of the electron transport chain, UQCRC1, are mitochondrial proteins that regulate TLR7/9-specific innate regulatory responses. Interestingly, PDK2 also regulates the glycolytic production of pyruvate and triggers upregulation of the transcription factor HIF-1α, providing a potential link between innate immune and glycolytic regulation of HIF-1α transcription (Sun et al., 2009). We also demonstrate that PDK2 can physically associate with IRAK1, TRAF6, and TAK1, suggesting that endosomal MyD88-dependent signaling events are reliant upon an intermediate mitochondrial complex containing PDK2 and other membrane-spanning proteins. Taken together, these data highlight the expanding role for cellular organelles as platforms for host defense and innate signaling responses.

TLR7/9 Cofactors in SLE and Immune Diseases

Importantly, 138 genes identified in our RNAi screen have been previously associated with genetic or gene expression variations (by GWAS or microarray, respectively) that underlie autoimmune or infection-related phenotypes. One autoimmune disorder, systemic lupus erythematosus (SLE), is characterized by the production of autoantibodies directed at nuclear antigens; genetic and experimental evidence suggests that deregulated innate immune responses can trigger this autoimmune disease (Waldner, 2009). Intriguingly, our analysis identified a number of molecular components associated with SLE disease onset or pathology as regulators of TLR signaling, including nuclear autoantigens (histones H2A, H2B, and SNRPD3 [Sm-D]), a regulator of antigen presentation (CD40), and a mediator of complement response (C4b) (Cook and Botto, 2006; Zieve and Khusial, 2003). These findings support a hypothesis that SLE autoantigens may also act as "endogenous-adjuvants."

In addition, this analysis identified PHRF1 (also known as KIAA1542) as an essential regulator of the transcriptional response to TLR7/9 activation. A genome-wide association scan identified a single nucleotide polymorphism in an intronic region of *PHRF1* (rs4963128) that was strongly linked to patients with SLE (Harley et al., 2008). This polymorphism is 23 kb telomeric to *IRF7*, and the two loci are in strong linkage disequilibrium. As a consequence, it has been suggested that deregulation of IRF7 may result in the production of specific autoantibodies (Salloum et al., 2010). However, a functional link between PHRF1 and TLR7 signaling responses supports the possibility that variations in PHRF1 activity may play a causal role in the onset of SLE.

HRS and TLR7/9 Trafficking

HRS is a proximal component of the endosomal sorting complex required for transport (ESCRT) machinery; we find that HRS is required for proper trafficking of TLR7/9 to endolysosomal networks, supporting a positive role for an upstream component of the ESCRT machinery in endosomal receptor sorting. Interestingly, *Drosophila* HRS was also recently shown to be necessary for robust signaling of the ancestral Toll pathway (Huang et al., 2010).

In classical models of ESCRT-mediated protein trafficking, activated receptors are downregulated from the plasma membrane, packaged into MVBs, and ultimately degraded as MVBs fuse with lysosomes (Hanson et al., 2009). Such negative regulation has been observed for TLRs: for example, TLR4 is ubiquitinated, interacts with HRS, and is degraded following LPS sensing (Husebye et al., 2006). As our results show a weak interaction between HRS and TLR2, it is possible that additional plasma membrane-associated TLRs, including TLR2, are regulated in a similar manner. In contrast to this model, we show that TLR9 is positively regulated via a physical interaction with HRS, and that this association leads to delivery of the receptor to the endolysosome, enabling signaling responses, instead of favoring protein degradation. We show these events are also dependent on the ubiquitination of TLR9 in a post-ER compartment; this modification of the receptor permits a highly specific interaction with HRS that is critical for TLR9 activation, since mutation of only three lysine residues impairs receptor interaction with HRS, as well as trafficking, processing, and signaling. Importantly, previous studies have shown that the impairment of HRS function does not disrupt endosome formation or acidification (Bache et al., 2003; Vaccari et al., 2010). Together with our observation that both mutations of the TLR9 cytoplasmic lysines and depletion of HRS result in similar defects in receptor trafficking, these data support a unique role for HRS in the ubiquitin-dependent targeting of TLR9 to the endosome.

We further hypothesize that the targeting of TLR7/9 to endolysosomes by HRS is dependent on a noncanonical ESCRT pathway, because TLR7/9 would not be able to signal from intralumenal vesicles within MVBs and would be targeted for lysosomal degradation. This is consistent with evidence also suggesting that, in some cases, HRS or ESCRT complexes may govern sorting steps that do not result in receptor degradation. For example, HRS directs recycling of the β2-adrenergic receptor to the plasma membrane (Hanyaloglu et al., 2005), and ESCRT-I promotes sorting of Tyrp1 from early endosomes to melanosomes (Truschel et al., 2009). Taken together, our results support a role for HRS in ubiquitin-dependent, nondegradative TLR7/9 receptor trafficking; further studies will be required to elucidate the potential noncanonical role of the ESCRT pathway in the processing and lysosomal trafficking of TLR9.

Based upon the integration of RNAi, proteomic, and gene expression data sets, this study provides a comprehensive systems-level analysis of the MyD88-dependent signaling response to endosomal nucleic acids. Secondary genetic and biochemical analyses enabled the modeling of an extended signaling network hierarchy that mediates the transcriptional response to TLR7/9 activation, and defined roles for proteins involved in ubiquitination and proteasomal degradation, chromatin remodeling, ancient stress responses, and receptor trafficking in the regulation of innate immune signaling responses. Recently, a study describing a systematic survey of TLR-responsive genes reported 280 putative innate immune signaling components (Chevrier et al., 2011). We observed limited overlap between the factors identified by Chevrier et al. and the TLR7/9 cofactors described here (data not shown). This discrepancy may be attributable to the differences in underlying experimental approaches, but additionally suggests that genetic screens have not reached saturation and that additional TLR regulatory components remain to be discovered. In total, our study provides global insight toward the molecular circuits that govern the cellular response to microbial infection, and identifies therapeutic targets for the treatment of autoimmunity and microbial infection.

EXPERIMENTAL PROCEDURES

Reagents

Latex beads were purchased from Polysciences. Human CpG oligonucleotides, murine CpG oligonucleotides (TCCATGACGTTCCTGACGTT) with phosphorothioate linkages, and all primers used for RT-PCR were from IDT. R848 and flagellin were purchased from Invivogen. Human TNF-α, human IL-1β, and antibodies against HA, MYC, ubiquitin, IκBα, tubulin, and β-actin were from Cell Signaling Technology; p65 antibody was from Santa Cruz Biotechnology; goat anti-mouse Alexa 488 secondary antibody was from Invitrogen; anti-FLAG antibody was from Sigma; anti-HRS antibody was from Abcam.

Cell Lines, Plasmids, and Tissue Culture

The HEK293T/TLR7/NF-κB and HEK293T/TLR9/NF-κB reporter cell lines were generated by transfecting HEK293T cells with TLR7 or TLR9 expression vectors, along with a 5× NF-κB luciferase reporter construct. HEK293T/TLR7/NF-κB and the HEK293T/TLR9/NF-κB cell lines were cultured in DMEM supplemented with 10% FBS (Thermo Scientific), L-glutamine, and penicillin/streptomycin, with the addition of 5 μg/ml of Blasticidin and 2 μg/ml of puromycin. RAW264.7 cells purchased from ATCC were cultured in RPMI supplemented with 10% FBS, L-glutamine, and penicillin/streptomycin. RAW264.7-TLR9-HA stable line was generated as described (Ewald et al., 2008). *TLR9*$^{-/-}$ immortalized macrophages expressing either WT-TLR9-HA or a KallR-TLR9-HA were generated by retroviral transduction using the MSCV2.2 vector. RAW264.7-TLR9-HA cells were transduced with LMP microRNA-adapted retroviral vectors (Thermo Scientific) targeting luciferase, *UNC93B1*, or *HRS* to generate stable knockdown cell lines. The WT-TLR9-HA and KallR-TLR9-HA expression vectors used in coimmunoprecipitation experiments were obtained by subcloning WT-TLR9-HA from MSCV2.2 retroviral vector into pCDNA3.1 vector.

Immunoprecipitation and Immunoblot Analysis

HEK293T cells were transiently transfected with expression vectors using Lipofectamine 2000 (Invitrogen). Forty-eight hours posttransfection, the cells were lysed (50 mM Tris-HCl [pH 7.4], 250 mM NaCl, 1 mM EDTA, 1% TRITON-100, supplemented with a complete protease inhibitor cocktail and phosphatase inhibitor cocktail [Sigma]). FLAG-HRS was immunoprecipitated using Dynabeads coated with protein G according to manufacturer's protocol (Invitrogen). For immunoblotting with ubiquitin antibody, RIPA buffer (25 mM Tris-HCl [pH 7.6], 150 mM NaCl, 1% NP-40, 1% sodium deoxycholate, 0.1% SDS) was supplemented with 40 mM N-ethylmaleimide.

p65 Translocation Assay

HEK293T/TLR7/NF-κB reporter cells were transfected with siRNAs. Three days posttransfection, the cells were stimulated with 1 μM of R848 for 40 min. The cells were fixed with 1% paraformaldehyde and then permeabilized and blocked using 0.3% TRITON-100 and 10% goat serum. Cells were then incubated overnight with a mouse anti-p65 antibody at 1:400 dilution. After three washes, cells were incubated for 1 hr with a goat anti-mouse Alexa

488 secondary antibody. Finally, cells were washed three more times and stained with Draq5.

ELISA

HEK293T/TLR7/NF-κB reporter cells were transfected with siRNAs. Three days posttransfection, transfectants were stimulated with 3 μM of R848 for 12 hr. Human IL-8 immunoassay (eBioscience, catalog number 88-8086) was performed according to the manufacturer's instructions.

Sendai Virus Infection

HEK293/TLR7/NF-κB reporter cells were reverse transfected with siRNAs. Seventy-two hours posttransfection, the media was removed and 25 μl of RPMI containing the appropriate amount of SeV was added (9 HA units). SeV was grown in 9-day-old embryonated chicken eggs (Spafas Charles River) and was titrated by hemagglutination assay (HA) using chicken red blood cells (Lampire Biological Laboratories). After infection, the plates were incubated for 45 min at 37°C. Then, 75 μl of RPMI with 10% FBS was added, cells were incubated at 37°C for an additional 10 hr, and the luciferase assay was performed.

More detail regarding the procedures outlined here, as well as additional experimental procedures, can be found in the Supplemental Experimental Procedures.

SUPPLEMENTAL INFORMATION

Supplemental Information includes Supplemental Experimental Procedures, Supplemental References, four figures, and seven tables and can be found with this article online at doi:10.1016/j.chom.2012.02.002.

ACKNOWLEDGMENTS

This work was supported in part by the Defense Threat Reduction Agency Joint Science and Technology Office (DTRA-JSTO) contract HDTRA1-07-9-0001 from the Department of Defense Chemical and Biological Defense program through the Defense Threat Reduction Agency (DTRA). The work is also supported by an Alliance for Lupus Research Grant, San Diego Center for Systems Biology (grant P50GM085764), National Institutes of Health (NIH) F31 grant AG032171 (to A.M.O.), the Irvington Institute Fellowship Program of the Cancer Research Institute (to A.E.), NIH/National Institute of Allergy and Infectious Diseases (NIAID) grant P01 AI090935 (HIV immune networks team, HINT), and NIH grant AI77780. The authors thank the Small Molecule Immune Potentiators (SMIP) team at Novartis for helpful discussions.

Received: August 23, 2011
Revised: December 4, 2011
Accepted: February 6, 2012
Published: March 14, 2012

REFERENCES

Akira, S., Uematsu, S., and Takeuchi, O. (2006). Pathogen recognition and innate immunity. Cell *124*, 783–801.

Arpaia, N., Godec, J., Lau, L., Sivick, K.E., McLaughlin, L.M., Jones, M.B., Dracheva, T., Peterson, S.N., Monack, D.M., and Barton, G.M. (2011). TLR signaling is required for *Salmonella typhimurium* virulence. Cell *144*, 675–688.

Bache, K.G., Brech, A., Mehlum, A., and Stenmark, H. (2003). Hrs regulates multivesicular body formation via ESCRT recruitment to endosomes. J. Cell Biol. *162*, 435–442.

Barton, G.M., Kagan, J.C., and Medzhitov, R. (2006). Intracellular localization of Toll-like receptor 9 prevents recognition of self DNA but facilitates access to viral DNA. Nat. Immunol. *7*, 49–56.

Blasius, A.L., and Beutler, B. (2010). Intracellular toll-like receptors. Immunity *32*, 305–315.

Blasius, A.L., Arnold, C.N., Georgel, P., Rutschmann, S., Xia, Y., Lin, P., Ross, C., Li, X., Smart, N.G., and Beutler, B. (2010). Slc15a4, AP-3, and Hermansky-Pudlak syndrome proteins are required for Toll-like receptor signaling in plasmacytoid dendritic cells. Proc. Natl. Acad. Sci. USA *107*, 19973–19978.

Carmeliet, P., Dor, Y., Herbert, J.M., Fukumura, D., Brusselmans, K., Dewerchin, M., Neeman, M., Bono, F., Abramovitch, R., Maxwell, P., et al. (1998). Role of HIF-1alpha in hypoxia-mediated apoptosis, cell proliferation and tumour angiogenesis. Nature *394*, 485–490.

Chevrier, N., Mertins, P., Artyomov, M.N., Shalek, A.K., Iannacone, M., Ciaccio, M.F., Gat-Viks, I., Tonti, E., DeGrace, M.M., Clauser, K.R., et al. (2011). Systematic discovery of TLR signaling components delineates viral-sensing circuits. Cell *147*, 853–867.

Chuang, T.H., and Ulevitch, R.J. (2004). Triad3A, an E3 ubiquitin-protein ligase regulating Toll-like receptors. Nat. Immunol. *5*, 495–502.

Cinque, B., Di Marzio, L., Centi, C., Di Rocco, C., Riccardi, C., and Grazia Cifone, M. (2003). Sphingolipids and the immune system. Pharmacol. Res. *47*, 421–437.

Conze, D.B., Wu, C.J., Thomas, J.A., Landstrom, A., and Ashwell, J.D. (2008). Lys63-linked polyubiquitination of IRAK-1 is required for interleukin-1 receptor- and toll-like receptor-mediated NF-kappaB activation. Mol. Cell. Biol. *28*, 3538–3547.

Cook, H.T., and Botto, M. (2006). Mechanisms of Disease: the complement system and the pathogenesis of systemic lupus erythematosus. Nat. Clin. Pract. Rheumatol. *2*, 330–337.

Ewald, S.E., Lee, B.L., Lau, L., Wickliffe, K.E., Shi, G.P., Chapman, H.A., and Barton, G.M. (2008). The ectodomain of Toll-like receptor 9 is cleaved to generate a functional receptor. Nature *456*, 658–662.

Hanson, P.I., Shim, S., and Merrill, S.A. (2009). Cell biology of the ESCRT machinery. Curr. Opin. Cell Biol. *21*, 568–574.

Hanyaloglu, A.C., McCullagh, E., and von Zastrow, M. (2005). Essential role of Hrs in a recycling mechanism mediating functional resensitization of cell signaling. EMBO J. *24*, 2265–2283.

Harley, J.B., Alarcon-Riquelme, M.E., Criswell, L.A., Jacob, C.O., Kimberly, R.P., Moser, K.L., Tsao, B.P., Vyse, T.J., Langefeld, C.D., Nath, S.K., et al. (2008). Genome-wide association scan in women with systemic lupus erythematosus identifies susceptibility variants in ITGAM, PXK, KIAA1542 and other loci. Nat. Genet. *40*, 204–210.

Huang, H.R., Chen, Z.J., Kunes, S., Chang, G.D., and Maniatis, T. (2010). Endocytic pathway is required for Drosophila Toll innate immune signaling. Proc. Natl. Acad. Sci. USA *107*, 8322–8327.

Husebye, H., Halaas, O., Stenmark, H., Tunheim, G., Sandanger, O., Bogen, B., Brech, A., Latz, E., and Espevik, T. (2006). Endocytic pathways regulate Toll-like receptor 4 signaling and link innate and adaptive immunity. EMBO J. *25*, 683–692.

Kawai, T., and Akira, S. (2006). TLR signaling. Cell Death Differ. *13*, 816–825.

Kim, Y.M., Brinkmann, M.M., Paquet, M.E., and Ploegh, H.L. (2008). UNC93B1 delivers nucleotide-sensing toll-like receptors to endolysosomes. Nature *452*, 234–238.

Konig, R., Chiang, C.Y., Tu, B.P., Yan, S.F., DeJesus, P.D., Romero, A., Bergauer, T., Orth, A., Krueger, U., Zhou, Y., et al. (2007). A probability-based approach for the analysis of large-scale RNAi screens. Nat. Methods *4*, 847–849.

Konig, R., Stertz, S., Zhou, Y., Inoue, A., Hoffmann, H.H., Bhattacharyya, S., Alamares, J.G., Tscherne, D.M., Ortigoza, M.B., Liang, Y., et al. (2009). Human host factors required for influenza virus replication. Nature *463*, 813–817.

Kouzarides, T. (2007). Chromatin modifications and their function. Cell *128*, 693–705.

Kumar, H., Kawai, T., and Akira, S. (2011). Pathogen recognition by the innate immune system. Int. Rev. Immunol. *30*, 16–34.

Machleidt, T., Kramer, B., Adam, D., Neumann, B., Schutze, S., Wiegmann, K., and Kronke, M. (1996). Function of the p55 tumor necrosis factor receptor "death domain" mediated by phosphatidylcholine-specific phospholipase C. J. Exp. Med. *184*, 725–733.

Maxwell, P.H., Wiesener, M.S., Chang, G.W., Clifford, S.C., Vaux, E.C., Cockman, M.E., Wykoff, C.C., Pugh, C.W., Maher, E.R., and Ratcliffe, P.J. (1999). The tumour suppressor protein VHL targets hypoxia-inducible factors for oxygen-dependent proteolysis. Nature *399*, 271–275.

Melchjorsen, J., Jensen, S.B., Malmgaard, L., Rasmussen, S.B., Weber, F., Bowie, A.G., Matikainen, S., and Paludan, S.R. (2005). Activation of innate defense against a paramyxovirus is mediated by RIG-I and TLR7 and TLR8 in a cell-type-specific manner. J. Virol. *79*, 12944–12951.

Mouchess, M.L., Arpaia, N., Souza, G., Barbalat, R., Ewald, S.E., Lau, L., and Barton, G.M. (2011). Transmembrane mutations in Toll-like receptor 9 bypass the requirement for ectodomain proteolysis and induce fatal inflammation. Immunity *35*, 721–732.

Park, B., Brinkmann, M.M., Spooner, E., Lee, C.C., Kim, Y.M., and Ploegh, H.L. (2008). Proteolytic cleavage in an endolysosomal compartment is required for activation of Toll-like receptor 9. Nat. Immunol. *9*, 1407–1414.

Paun, A., Reinert, J.T., Jiang, Z., Medin, C., Balkhi, M.Y., Fitzgerald, K.A., and Pitha, P.M. (2008). Functional characterization of murine interferon regulatory factor 5 (IRF-5) and its role in the innate antiviral response. J. Biol. Chem. *283*, 14295–14308.

Saksena, S., Sun, J., Chu, T., and Emr, S.D. (2007). ESCRTing proteins in the endocytic pathway. Trends Biochem. Sci. *32*, 561–573.

Salloum, R., Franek, B.S., Kariuki, S.N., Rhee, L., Mikolaitis, R.A., Jolly, M., Utset, T.O., and Niewold, T.B. (2010). Genetic variation at the IRF7/PHRF1 locus is associated with autoantibody profile and serum interferon-alpha activity in lupus patients. Arthritis Rheum. *62*, 553–561.

Sasai, M., Linehan, M.M., and Iwasaki, A. (2010). Bifurcation of Toll-like receptor 9 signaling by adaptor protein 3. Science *329*, 1530–1534.

Sepulveda, F.E., Maschalidi, S., Colisson, R., Heslop, L., Ghirelli, C., Sakka, E., Lennon-Dumenil, A.M., Amigorena, S., Cabanie, L., and Manoury, B. (2009). Critical role for asparagine endopeptidase in endocytic Toll-like receptor signaling in dendritic cells. Immunity *31*, 737–748.

Seth, R.B., Sun, L., Ea, C.K., and Chen, Z.J. (2005). Identification and characterization of MAVS, a mitochondrial antiviral signaling protein that activates NF-kappaB and IRF 3. Cell *122*, 669–682.

Simon, D., and Ferretti, J.J. (1991). Electrotransformation of Streptococcus pyogenes with plasmid and linear DNA. FEMS Microbiol. Lett. *66*, 219–224.

Su, A.I., Cooke, M.P., Ching, K.A., Hakak, Y., Walker, J.R., Wiltshire, T., Orth, A.P., Vega, R.G., Sapinoso, L.M., Moqrich, A., et al. (2002). Large-scale analysis of the human and mouse transcriptomes. Proc. Natl. Acad. Sci. USA *99*, 4465–4470.

Sun, W., Zhou, S., Chang, S.S., McFate, T., Verma, A., and Califano, J.A. (2009). Mitochondrial mutations contribute to HIF1alpha accumulation via increased reactive oxygen species and up-regulated pyruvate dehydrogenease kinase 2 in head and neck squamous cell carcinoma. Clin. Cancer Res. *15*, 476–484.

Takeuchi, O., and Akira, S. (2010). Pattern recognition receptors and inflammation. Cell *140*, 805–820.

Tannahill, G.M., and O'Neill, L.A. (2011). The emerging role of metabolic regulation in the functioning of Toll-like receptors and the NOD-like receptor Nlrp3. FEBS Lett. *585*, 1568–1572.

Truschel, S.T., Simoes, S., Setty, S.R., Harper, D.C., Tenza, D., Thomas, P.C., Herman, K.E., Sackett, S.D., Cowan, D.C., Theos, A.C., et al. (2009). ESCRT-I function is required for Tyrp1 transport from early endosomes to the melanosome limiting membrane. Traffic *10*, 1318–1336.

Vaccari, T., Duchi, S., Cortese, K., Tacchetti, C., and Bilder, D. (2010). The vacuolar ATPase is required for physiological as well as pathological activation of the Notch receptor. Development *137*, 1825–1832.

Waldner, H. (2009). The role of innate immune responses in autoimmune disease development. Autoimmun. Rev. *8*, 400–404.

Wegner, C.S., Rodahl, L.M., and Stenmark, H. (2011). ESCRT proteins and cell signalling. Traffic *12*, 1291–1297.

Yoneyama, M., Kikuchi, M., Natsukawa, T., Shinobu, N., Imaizumi, T., Miyagishi, M., Taira, K., Akira, S., and Fujita, T. (2004). The RNA helicase RIG-I has an essential function in double-stranded RNA-induced innate antiviral responses. Nat. Immunol. *5*, 730–737.

Zhou, Y., Young, J.A., Santrosyan, A., Chen, K., Yan, S.F., and Winzeler, E.A. (2005). In silico gene function prediction using ontology-based pattern identification. Bioinformatics *21*, 1237–1245.

Zieve, G.W., and Khusial, P.R. (2003). The anti-Sm immune response in autoimmunity and cell biology. Autoimmun. Rev. *2*, 235–240.

Zinkernagel, A.S., Hruz, P., Uchiyama, S., von Kockritz-Blickwede, M., Schuepbach, R.A., Hayashi, T., Carson, D.A., and Nizet, V. (2011). Importance of Toll-like receptor 9 in host defense against M1T1 group A Streptococcus infections. J. Innate. Immun. *4*, 213–218.